

## Conductive Behavior of High TiO<sub>2</sub> Nanoparticle Content of Inorganic/Organic Nanostructured Composites

Junkal Gutierrez, Agnieszka Tercjak,\* and Iñaki Mondragon\*

“Materials + Technologies” Group, Departamento de Ingeniería Química y Medio Ambiente, Escuela Politecnica, Universidad Pais Vasco/Euskal Herriko Unibertsitatea, Pza. Europa 1, 20018 Donostia-San Sebastian, Spain

Received October 1, 2009; E-mail: agnieszka.tercjaks@ehu.es; inaki.mondragon@ehu.es

**Abstract:** Amphiphilic polystyrene-*b*-poly(ethylene oxide) (PS-*b*-PEO) diblock copolymers with different block ratios were used as templates for the incorporation of a high content of titanium dioxide nanoparticles using the sol–gel method. Confinement of the inorganic part in the PEO block of the block copolymer allows the generation of nanostructured systems with a high nanoparticle content. As successfully demonstrated using tunneling atomic force microscopy, the investigated systems maintained the conductive properties of the TiO<sub>2</sub> nanoparticles. The obtained results confirmed that with increasing TiO<sub>2</sub> nanoparticle content, the local current value increased up to 15 pA, and this conductivity value strongly depended on the amount of the PEO block in the block copolymer template. Moreover, the results indicated that control of the ratio between the sol–gel and the PEO block allows the design of well-dispersed, conductive inorganic/organic hybrids with high inorganic content. These materials can provide attractive strategies in the field of dye-sensitized solar cells.

### Introduction

At the present time, block-copolymer-based materials have attracted much attention in view of their potential applications, since the self-assembly capacity of this kind of material with nanoscale periodicity allows the creation of nanopatterned materials.<sup>1–4</sup> Several studies have reported the use of block copolymers as templates for the synthesis of nanostructured materials because of their ability to control both the size and the spatial organization by varying their composition and molecular weight.<sup>5,6</sup>

On the other hand, nanostructures of semiconductors and metals have been extensively studied in recent years because of their unique magnetic, optical, electrical, and catalytic properties and their potential applications in the field of nanotechnology.<sup>7–10</sup> It is well-known that the properties of such nanostructured materials depend strongly on the size, shape, and composition.<sup>11,12</sup> In particular, titanium dioxide nanoparticles

have received considerable interest because of their large surface areas and wide application in the fields of dye-sensitized solar cells (DSSC)<sup>13–17</sup> and electric and photocatalytic systems.<sup>18,19</sup> Extensive work involving methods for obtaining metal nanoparticles selectively incorporated within one of the microdomains of block copolymers has been reported.<sup>7,8,20</sup> The sol–gel method is a simple fabrication protocol for synthesizing nanoparticles with well-defined sizes. However, all of the parameters must be strictly controlled, since a small change in one of the parameters, such as temperature, reaction time, or concentration, can significantly influence the results.<sup>21</sup> In this study, the sol–gel method has been used for the synthesis of inorganic/organic nanostructured composites based on titanium dioxide nanoparticles. Two different molecular weight polystyrene-*b*-poly(ethylene oxide) (PS-*b*-PEO) block copolymers have been used as templating agents. These amphiphilic block copolymers allow the synthesis to be performed without using any type of surfactant since the generated sol–gel solution

- (1) Hamley, I. W. *Prog. Polym. Sci.* **2009**, in press.
- (2) Li, M.; Ober, C. K. *Mater. Today* **2006**, *9*, 30–39.
- (3) Olson, D. A.; Chen, L.; Hillmyer, M. A. *Chem. Mater.* **2008**, *20*, 869–890.
- (4) Darling, S. B. *Surf. Sci.* **2007**, *601*, 2555–2561.
- (5) Grosso, D.; Cagnool, F.; Soler-Illia, G. J. D. A.; Crepaldi, E. L.; Amenitsch, H.; Bruneau, A.; Bourgeois, A.; Sanchez, C. *Adv. Funct. Mater.* **2004**, *14*, 309–322.
- (6) Hamley, I. W. *The Physics of Block Copolymers*; Oxford University Press: New York, 1998.
- (7) García, I.; Tercjak, A.; Zafeiropoulos, N. E.; Stamm, M.; Mondragon, I. *Macromol. Rapid Commun.* **2007**, *28*, 2361–2365.
- (8) Peponi, L.; Tercjak, A.; Gutierrez, J.; Stadler, H.; Torre, L.; Kenny, J. M.; Mondragon, I. *Macromol. Mater. Eng.* **2008**, *293*, 568–573.
- (9) Zhao, Y.; Zhai, J.; Wei, T.; Jiang, L.; Zhu, D. *J. Mater. Chem.* **2007**, *17*, 5084–5089.
- (10) Calvo, M. E.; Colodrero, S.; Rojas, T. C.; Anta, J. A.; Ocaña, M.; Miguez, H. *Adv. Funct. Mater.* **2008**, *18*, 2708–2715.
- (11) Moriarty, P. *Rep. Prog. Phys.* **2001**, *64*, 297–381.

- (12) Almquist, C. B.; Biswas, P. *J. Catal.* **2002**, *212*, 145–156.
- (13) Pichot, F.; Pitts, J. R.; Gregg, B. A. *Langmuir* **2000**, *16*, 5626–5630.
- (14) Longo, C.; Nogueira, A. F.; De Paoli, M. A.; Cachet, H. *J. Phys. Chem. B* **2002**, *106*, 5925–5930.
- (15) Lindstrom, H.; Holmberg, A.; Magnusson, E.; Lindquist, S. E.; Malmqvist, L.; Hagfeldt, A. *Nano Lett.* **2001**, *1*, 97–100.
- (16) Lindstrom, H.; Hornberg, A.; Magnusson, E.; Malmqvist, L.; Hagfeldt, A. *J. Photochem. Photobiol. A* **2001**, *145*, 107–112.
- (17) Miyasaka, T.; Ikegami, M.; Kijitori, Y. *J. Electrochem. Soc.* **2007**, *154*, 455–462.
- (18) Baiju, K. V.; Periyat, P.; Wunderlich, W.; Pillai, P. K.; Mukundan, P.; Warriar, G. K. *J. Sol–Gel Sci. Technol.* **2007**, *43*, 283–290.
- (19) Alvaro, M.; Aprile, C.; Benitez, M.; Carbonell, E.; Garcia, H. *J. Phys. Chem. B* **2006**, *110*, 6661–6665.
- (20) Tercjak, A.; Gutierrez, J.; Ocando, C. J.; Peponi, L.; Mondragon, I. *Acta Mater.* **2009**, *57*, 4624–4631.
- (21) Brinker, C. J.; Scherer, G. W. *Sol–Gel Science: The Physics and Chemistry of Sol–Gel Processing*; Academic Press: Boston, 1990.

interacts with the hydrophilic PEO block, leading to the formation of hydrogen bonds.<sup>22</sup> Many approaches for the synthesis and characterization of nanostructured TiO<sub>2</sub>/PS-*b*-PEO nanocomposites have been reported.<sup>22–30</sup>

Herein, to the best of our knowledge, TiO<sub>2</sub>/PS-*b*-PEO nanocomposites with high amounts of inorganic component have been achieved for the first time without loss of the template nanostructure in the obtained inorganic/organic hybrid materials. As these types of systems may open the door to a wide range of possible applications in electronic nanodevices, tunneling atomic force microscopy (TUNA) has been successfully applied to investigate the charge distribution and conductivity level of the synthesized nanocomposites. TUNA measurements were performed because this technique offers a unique ability to determine local ultralow current values on inorganic/organic materials at the nanoscale level. On the basis of the obtained TUNA current images under an applied voltage, we demonstrate that well-dispersed and closely packed TiO<sub>2</sub> nanoparticles can be used for designing nanostructured conductive materials.

### Experimental Section

**Materials.** The sol–gel solution used to obtain the TiO<sub>2</sub> nanoparticles was prepared using titanium isopropoxide (TTIP) as the precursor. It was purchased from Sigma-Aldrich. Analytical-grade toluene, isopropyl alcohol, and hydrochloric acid (HCl, 37%) were purchased from Sigma-Aldrich. Two PS-*b*-PEO diblock copolymers with high (HSEO) and low (LSEO) PS block contents ( $M_n^{PS} = 125\,000$  g/mol,  $M_n^{PEO} = 16\,100$  g/mol,  $M_w/M_n = 1.4$  for HSEO;  $M_n^{PS} = 58\,600$  g/mol,  $M_n^{PEO} = 31\,000$  g/mol,  $M_w/M_n = 1.03$  for LSEO) were purchased from Polymer Source, Inc.

TiO<sub>2</sub>/PS-*b*-PEO nanocomposites were synthesized following the preparation method published by Sun and co-workers,<sup>23,24</sup> Cheng and co-workers,<sup>27,28</sup> and Gutierrez et al.<sup>22</sup> First, HSEO or LSEO block copolymer solutions (10 wt %) were dissolved in toluene. Next, the sol–gel solution was prepared by adding isopropyl alcohol (5 mL), TTIP (0.125 mmol), and HCl (0.125 mmol). Subsequently, toluene (5 mL) was dropped slowly into the homogeneous mixture of the sol–gel and stirred for 1 h. Afterward, the desired amount of sol–gel (30, 40, 50, or 60 vol % relative to the block copolymer amount) was added to the block copolymer solution and stirred for 30 min. Finally, the mixed solutions were filtered using a 0.2 μm PTFE filter. Hybrid inorganic/organic films were produced by spin-coating onto Si(100) wafers at 2000 rpm for 30 s using a Telstar Instrumat model P-6708D spin-coater.

To analyze the effect of sol–gel reaction time on the size of the generated TiO<sub>2</sub> nanoparticles in the nanocomposites, TiO<sub>2</sub>/LSEO samples were synthesized using various reaction times from 1 h to 2 months. In view of the similar morphologies of all of the synthesized nanocomposites for each sol–gel content used, the variation with reaction time is described only for the 40 vol % sol–gel/LSEO nanocomposite.



**Figure 1.** Transparency of TiO<sub>2</sub>/HSEO nanocomposite solutions containing 0, 10, 20, 30, 40, 50, and 60 vol % sol–gel.

**Techniques.** Weight fractions of TiO<sub>2</sub> in the inorganic/organic nanocomposites were measured by thermogravimetric analysis (TGA) using a TGA/SDTA-851e instrument under a nitrogen atmosphere at a heating rate of 10 °C min<sup>−1</sup> from room temperature to 700 °C.

Atomic force microscopy (AFM) was performed in tapping mode using a Dimension 3100 NanoScope IV (Veeco). Etched single-beam cantilever (110–140 μm length) silicon nitride probes having a nominal tip radius of 10 nm were used. Scan rates ranged from 0.7 to 1.2 Hz s<sup>−1</sup>. Measurements were performed with 512 scan lines and a target amplitude of ~0.9 V. In order to obtain repeatable results for the nanocomposite morphology, different regions of the specimens were scanned.

TUNA analysis was performed under ambient conditions using a Veeco Dimension 3100 scanning probe microscope equipped with a Nanoscope IVa controller and a TUNA extension module. The TUNA current-sensing range is sensitive to low currents (50 fA to 100 pA), while the TUNA extension module allows the measurement of higher currents (up to 1000 nA). For the TUNA measurements, nanocomposite films were prepared using indium tin oxide (ITO)-coated glass substrates. All of the TUNA measurements were carried out in contact mode using a conductive Co/Cr-coated MESP tip having a resonance frequency of ~75 kHz and a cantilever spring constant of ~40 N/m. In order to obtain repeatable results, local electrical properties of the investigated samples were measured in different regions of the specimens. Similar TUNA images were obtained, thus demonstrating the reproducibility of the results.

### Results and Discussion

The transparencies of nanocomposite solutions without sol–gel and with various sol–gel contents are shown in Figure 1. As can be seen, the opacity of the investigated solutions changed with increasing sol–gel amount. The digital photographs of the 10 and 20 vol % nanocomposite solutions were added to Figure 1 only in order to better understand the transparency behavior of TiO<sub>2</sub>/HSEO nanocomposites. The synthesis and characterization of these nanocomposites has been previously reported by us.<sup>22</sup> As can be seen, the opacity increased up to a sol–gel content of 30 vol %, and thereafter the solutions became more transparent with increasing sol–gel content. The highest transparency was reached for the 60 vol % sol–gel/HSEO nanocomposite solution. Since the amount (vol %) of block copolymer in

**Table 1.** Weight Fractions (wt %) of TiO<sub>2</sub> and the PEO Block in TiO<sub>2</sub>/HSEO and TiO<sub>2</sub>/LSEO Nanocomposites as Functions of the Amount of the Sol–Gel Volume Fraction Added in the Synthesis, As Determined by TGA

sol–gel vol %	in TiO <sub>2</sub> /HSEO		in TiO <sub>2</sub> /LSEO	
	TiO <sub>2</sub>	PEO block	TiO <sub>2</sub>	PEO block
30	36.7	7.2	36.1	41.8
40	45.9	6.2	46.2	35.2
50	51.8	5.5	52.5	31.1
60	66.5	3.8	66.8	21.7

- (22) Gutierrez, J.; Tercjak, A.; Garcia, I.; Peponi, L.; Mondragon, I. *Nanotechnology* **2008**, *19*, 155607.
- (23) Sun, Z.; Kim, D. H.; Wolkenhauer, M.; Bumbu, G. G.; Knoll, W.; Gutmann, J. S. *ChemPhysChem* **2006**, *7*, 370–378.
- (24) Sun, Z.; Wolkenhauer, M.; Bumbu, G. G.; Kim, D. H.; Gutmann, J. S. *Physica B* **2005**, *357*, 141–143.
- (25) Kim, D. H.; Kim, S. H.; Lavery, K.; Russell, T. P. *Nano Lett.* **2004**, *4*, 1841–1844.
- (26) Li, X.; Yang, H.; Li, C.; Xu, L.; Zhang, Z.; Kim, D. H. *Polymer* **2008**, *49*, 1376–1384.
- (27) Cheng, Y. J.; Gutmann, J. S. *J. Am. Chem. Soc.* **2006**, *128*, 4658–4674.
- (28) Cheng, Y. J.; Zhou, S.; Gutmann, J. S. *Macromol. Rapid Commun.* **2007**, *28*, 1392–1396.
- (29) Gutierrez, J.; Tercjak, A.; Peponi, L.; Mondragon, I. *J. Phys. Chem. C* **2009**, *113*, 8601–8605.
- (30) Li, X.; Peng, J.; Kang, J. H.; Choy, J. H.; Steinhart, M.; Knoll, W.; Kim, D. H. *Soft Matter* **2008**, *4*, 515–521.

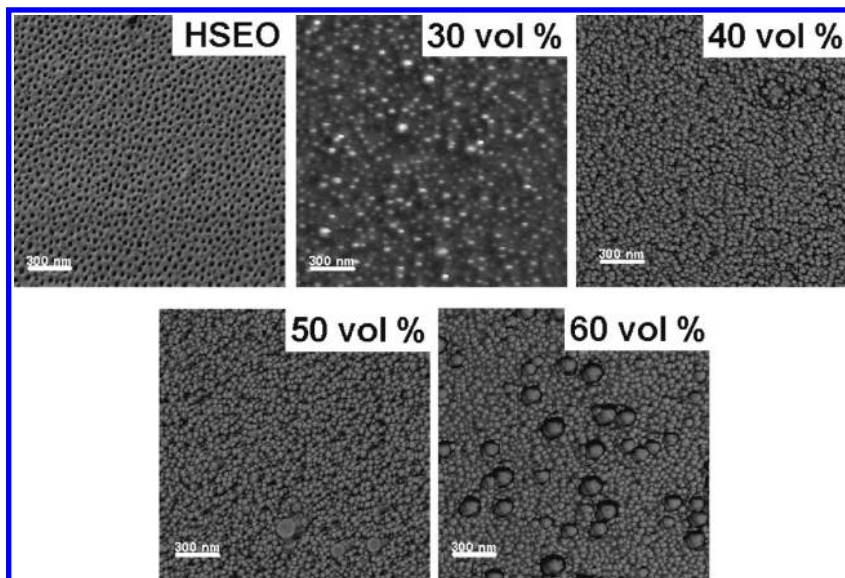


**Figure 2.** AFM phase images for HSEO, and different TiO<sub>2</sub>/HSEO nanocomposites obtained by varying the amount (vol %) of sol–gel.

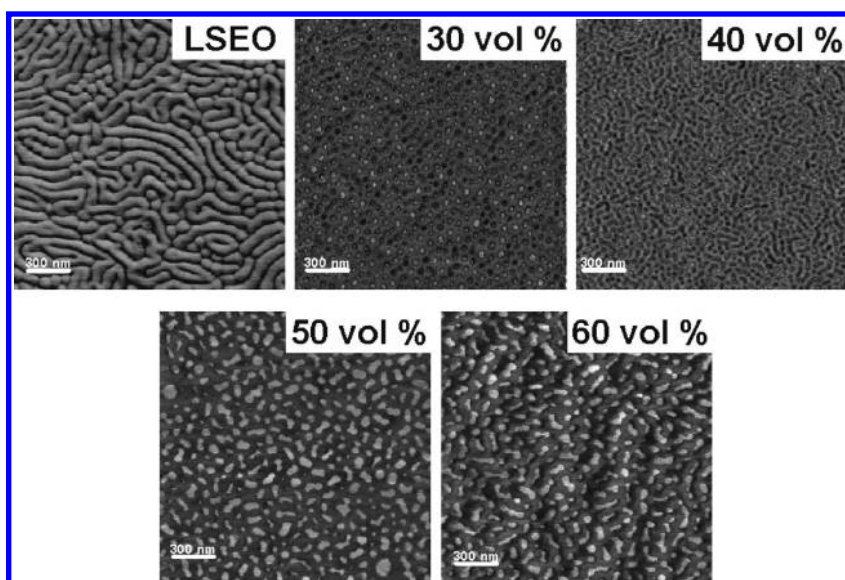


**Figure 3.** AFM phase images of LSEO and different TiO<sub>2</sub>/LSEO nanocomposites obtained by varying the amount (vol %) of sol–gel.

the toluene solutions was constant, the transparency of the solutions depended on the volume ratio of the sol–gel and PEO block (since only the PEO block can interact with sol–gel<sup>22</sup>). Similar behavior was observed by Li et al.<sup>31</sup> They demonstrated that increasing the sol–gel content in sol–gel/epoxy nanocomposites resulted in a high transparency level despite the fact that samples with low sol–gel concentration were translucent. They indicated that this behavior can be related to nanoparticle dispersion, particle–polymer interface, and particle–polymer refractive index differences. A similar correlation can be found for our system, since the transparency level has a strong influence on the morphology generated in the investigated nanocomposites, as described below.

The content of titanium dioxide introduced into the HSEO and LSEO block copolymers after filtration and solvent evaporation was determined, taking into account the residue left after

thermal treatment from 25 to 750 °C. TGA results for all of the investigated TiO<sub>2</sub>/HSEO and TiO<sub>2</sub>/LSEO nanocomposite samples are listed in Table 1. As can be seen, for all of the TiO<sub>2</sub>/HSEO and TiO<sub>2</sub>/LSEO nanocomposites, the final inorganic content of both matrices was nearly constant for similar volumes of sol–gel used. Additionally, since TiO<sub>2</sub> nanoparticles interact with the PEO block, the weight fractions of this block are also given in Table 1.

AFM phase images of the HSEO block copolymer and TiO<sub>2</sub>/HSEO nanocomposites with different inorganic contents are shown in Figure 2. The neat HSEO spin-coated film presents a morphology between cubic and hexagonal,<sup>22,29</sup> with dark PEO block domains dispersed in the PS block matrix, which appears as lighter regions. As the vol % sol–gel increased, the diblock copolymer morphology was not significantly changed by the presence of the nanoparticles. For 30 vol % sol–gel, small bright dots can be clearly observed. These brighter spherical regions can be attributed to TiO<sub>2</sub> nanoparticles confined in the PEO block domains of the block copolymer. Nanocomposites syn-

(31) Li, Y. Q.; Fu, S. Y.; Yang, Y.; Mai, Y. W. *Chem. Mater.* **2008**, *20*, 2637–2643.

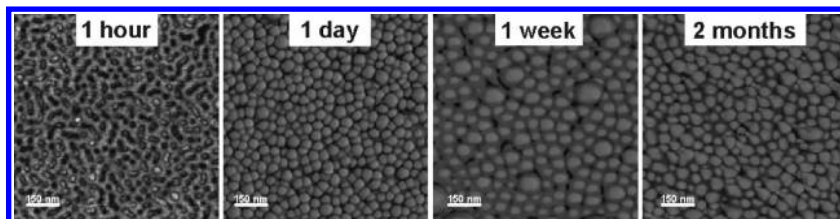


**Figure 4.** AFM phase images for 40 vol % sol-gel/LSEO nanocomposite synthesized using different sol-gel reaction times.

thesized with 40 and 50 vol % sol-gel showed similar morphologies with an increasing amount of nanoparticles. In both cases, the high inorganic content did not allow the PS block domains to be distinguished because TiO<sub>2</sub>/PEO block domains covered the surface. For these compositions, the diameter of individual spherical nanoparticles was between 50 and 60 nm. It is noteworthy that the 50 vol % sol-gel/HSEO nanocomposite exhibited some domains with larger diameter. This fact indicates that the amount of sol-gel used for generation of the TiO<sub>2</sub> nanoparticles was higher than the PEO block domains could accommodate. In the case of the 60 vol % sol-gel/HSEO nanocomposite, larger TiO<sub>2</sub> nanoparticle domains with a diameter of ~120 nm were detected, thus confirming that an excess of sol-gel provokes an increase in the size of the nanoparticle domains.

The addition of large amounts of TiO<sub>2</sub> nanoparticles into the LSEO block copolymer resulted in significant changes in morphology of the final nanocomposites. Figure 3 shows AFM phase images of the LSEO block copolymer and TiO<sub>2</sub>/LSEO nanocomposites with different inorganic contents. The neat

LSEO block copolymer showed a pseudolamellar morphology with a stripe spacing of ~65 nm.<sup>22</sup> Nanocomposites based on this block copolymer presented notable changes in the morphologies in comparison with the nanocomposites based on the HSEO block copolymer. The morphological structure of the neat LSEO block copolymer changed from lamellar to hexagonal for the 30 vol % sol-gel/LSEO nanocomposite, with center-to-center interval between cylinders of ~80 nm. TiO<sub>2</sub>-filled PEO block domains (bright domains) and unfilled PEO block domains (dark domains) can be clearly distinguished, thus indicating that the LSEO matrix could be almost filled with a higher concentration of nanoparticles. With increasing TiO<sub>2</sub> content, cylindrical TiO<sub>2</sub>/PEO block domains became more closely packed. This phenomenon is clearly observed in the case of the 40 vol % sol-gel/LSEO nanocomposite, for which one can even observe cylindrical domains merged into an interconnected wormlike structure. Here it should be pointed out that 40 vol % sol-gel was still not enough to fill all of the PEO block domains (dark domains). Nanocomposites synthesized using 50 and 60 vol % sol-gel showed very similar morphologies. In both cases, an

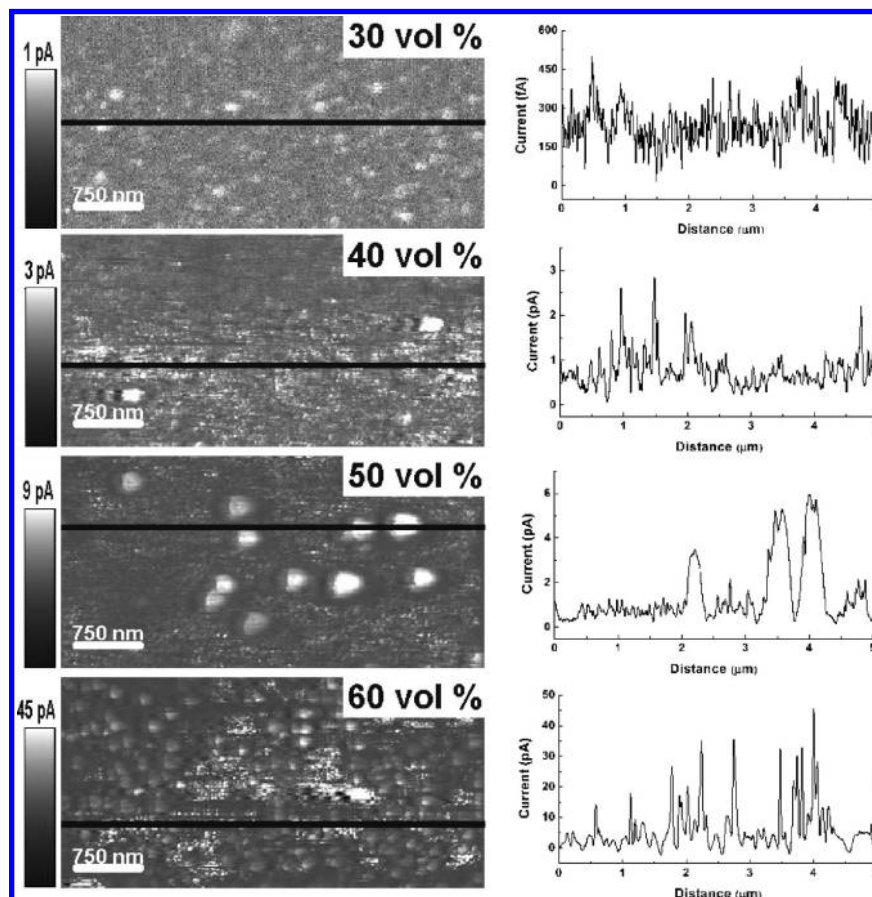


**Figure 5.** TUNA current images taken at a bias voltage of 10 V for different TiO<sub>2</sub>/HSEO nanocomposites obtained by varying the amount (vol %) of sol-gel.

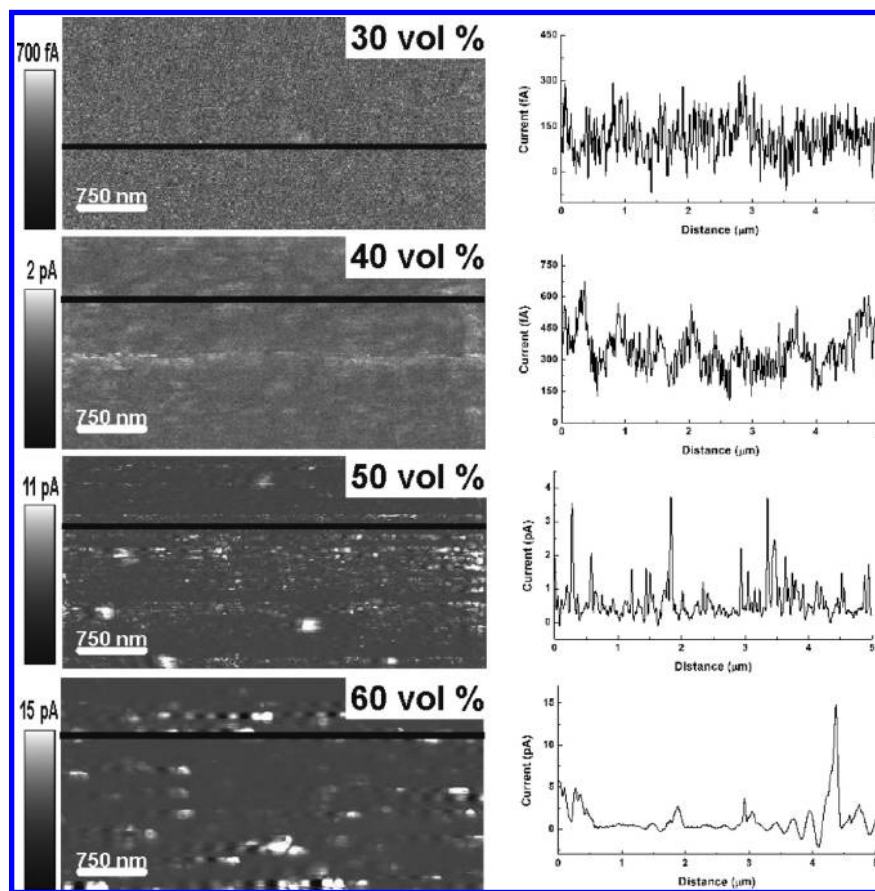


**Figure 6.** TUNA current images taken at a bias voltage of 10 V for different TiO<sub>2</sub>/LSEO nanocomposites obtained by varying the amount (vol %) of sol–gel.

interconnected wormlike structure with an average length of  $\sim 100$  nm was observed. These nanocomposites presented completely TiO<sub>2</sub>-filled PEO block bright domains in a PS block matrix.

Moreover, from a comparison of the morphology of the 60 vol % sol–gel/LSEO nanocomposite with that of the 60 vol % sol–gel/HSEO nanocomposite, it is worth noting that a larger amount of TiO<sub>2</sub> nanoparticles can be incorporated into the LSEO matrix since this block copolymer contains a larger amount of the PEO block, which is responsible for interactions with the sol–gel solution.<sup>22</sup> To conclude, in the case of the 60 vol % sol–gel/HSEO nanocomposite, the sol–gel content was so high that the generated TiO<sub>2</sub> domains were bigger than the PEO block domains. On the contrary, for the 60 vol % sol–gel/LSEO nanocomposite, the TiO<sub>2</sub> domains formed a well-defined wormlike structure.

It is well-known<sup>21,23,27</sup> that the morphologies of hybrid materials synthesized via the sol–gel method depend strongly on the type of template, concentration, pH, solvent, etc. On the other hand, the influence of the sol–gel reaction time on the final morphology of the nanocomposite was also investigated. Figure 4 shows AFM phase images of 40 vol % sol–gel/LSEO nanocomposites obtained using different sol–gel reaction times. An increase in the particle size from 30 to 50 nm was observed as the reaction time increased from 1 h to 2 months. The biggest particle size was reached for a reaction time of 1 week, after which nanoparticle/PEO domains with a diameter of  $\sim 60$  nm appeared. Additionally, as the reaction time increased, the morphology of the block copolymer matrix seemed to be very

similar. However, TiO<sub>2</sub> nanoparticles located in PEO block domains (TiO<sub>2</sub>/PEO domains) increased significantly.

As expected, the sol–gel reaction time study indicates a strong effect on the morphology generated in the nanocomposites. The morphology of a given vol % sol–gel nanocomposite changed from an interconnected wormlike structure for low synthesis times (30 min) to a hexagonal structure at longer times (1 day or longer). Moreover, it should be pointed out that neither the morphology nor nanoparticle size changed for synthesis times longer than 30 min. Therefore, one can conclude that the generated thin-film surfaces for reaction times longer than 1 h were covered by highly dense arrays of uniformly sized titanium dots.

The quantitative conductive behavior of the synthesized inorganic/organic nanocomposites on a nanometer scale was investigated using TUNA. This technique allows topographical and current images to be obtained at the same time. In the present study, the images were acquired with a bias voltage of 10 V between the AFM chuck and AFM tip. Since a good correlation between the simultaneously obtained topographical and current images was observed, the height images are not shown.

TUNA current images and the corresponding profiles of TiO<sub>2</sub>/HSEO nanocomposites with different inorganic contents are shown in Figure 5. It is worth noting that the conductivity of the films increased with increasing nanoparticle content in the nanocomposites. The conductivity values changed from 450 fA to 45 pA in going from the 30 to the 60 vol % sol–gel/HSEO nanocomposite. Additionally, here it should be pointed out that,

as is visible in the TUNA current images and corresponding profiles for the TiO<sub>2</sub>/HSEO nanocomposites, local higher-conductivity peaks were detected along the analyzed sample surface. The intensity of these peaks, corresponding to the bright domains in the TUNA current images, increased with increasing TiO<sub>2</sub> nanoparticle content in the nanocomposites. These results are in good agreement with the AFM results described above, indicating that the bright dots in the TUNA current images correspond to the TiO<sub>2</sub> nanoparticles in the AFM images.

TUNA current images and corresponding profiles for TiO<sub>2</sub>/LSEO nanocomposites are shown in Figure 6. In the case of TiO<sub>2</sub>/LSEO nanocomposites with lower inorganic content (30 vol %), no bright domains appeared in the TUNA current image, and the conductivity value, as marked in the corresponding profile, was ~450 fA. Thus, the current image was almost completely dark, indicating poor conductive behavior. On the contrary, increasing the TiO<sub>2</sub> nanoparticle content led to higher conductivity values (see the corresponding profiles), and consequently, small bright conductive domains appeared in the TUNA current images. TUNA measurements for the TiO<sub>2</sub>/LSEO nanocomposites, as well as for the TiO<sub>2</sub>/HSEO nanocomposites, indicated that the highest current values corresponded to the 60 vol % sol-gel/LSEO nanocomposite, which is related to the fact that these composites have the highest inorganic content. Here, once more it should be mentioned that the bright domains in the TUNA current images correspond to regions of higher conductivity, while the dark areas correspond to ultralow current. For the 60 vol % sol-gel/LSEO nanocomposite, the highest obtained current value was 15 pA.

Moreover, for all of the nanocomposite samples, in addition to the local high-current peaks, constant current values were detected from the whole sample surface. These current values increased with increasing inorganic content. This phenomenon was especially visible after deeper analysis of the TUNA current profiles and indicates that the applied voltage (10 V) provoked the current passing throughout the sample. Finally, comparing the conductivity values of the TiO<sub>2</sub>/HSEO and TiO<sub>2</sub>/LSEO nanocomposites, one can conclude that for all sample contents, nanocomposites based on the HSEO block copolymer are more conductive. This can be explained by taking into account the PEO content of the block copolymers. Since, as was previously

reported by us,<sup>22</sup> the PEO block interacts with the sol-gel solution, nanocomposites based on the HSEO block copolymer had a lower amount of PEO block able to lodge TiO<sub>2</sub> nanodots. Consequently, the obtained AFM morphologies corresponded to a surface covered by TiO<sub>2</sub> nanoparticles that was able to reach a higher level of conductivity. On the contrary, in the case of the LSEO block copolymer, the amount of PEO block was so high that even 60 vol % sol-gel was not enough to cover all of the PEO domains. As consequence, the current values in the case of the LSEO-based nanocomposites were lower.

## Conclusions

Inorganic/organic hybrid materials based on a high content of TiO<sub>2</sub> nanoparticles and polystyrene-*b*-poly(ethylene oxide) block copolymers as templates were studied. Well-defined nanostructured materials were obtained up to 60 vol % sol-gel content. TiO<sub>2</sub> nanodots confined onto the PEO block modified the final morphology generated in the nanocomposites. Generally, the morphology of the nanocomposites with the highest investigated vol % sol-gel changed from a structure between cubic and hexagonal pseudolamellar to a well-packed individual TiO<sub>2</sub> nanoparticle surface for the HSEO-based system and from a pseudolamellar to interconnected wormlike structure for the LSEO-based system. Moreover, TUNA results successfully demonstrated that well-dispersed TiO<sub>2</sub> nanodots had a strong effect on the conductivity of the designed materials. The conductivity of these systems increased with increasing TiO<sub>2</sub> content in the nanocomposites. These conductive, well-defined nanostructured inorganic/organic materials can find many possible applications, especially in the field of dye-sensitized solar cells.

**Acknowledgment.** Financial support from the Basque Country Government in the frame of Grupos Consolidados (IT-365-07) and the ETORTEK/inanoGUNE Project and from the Spanish Ministry of Education and Science (MAT2006-06331 and MAT2009-12832) is gratefully acknowledged. Additionally, J.G. thanks Eusko Jaurlaritza/Gobierno Vasco (Programas de becas para formación y perfeccionamiento de personal investigador) for the grant supplied for this work.

JA908359K